Editors' Suggestion

Aging of a quantum battery

Faezeh Pirmoradian[1,2] and Klaus Mølmer[2,*]

[1]*Department of Physics, Institute for Advanced Studies in Basic Sciences (IASBS), Zanjan 45137-66731, Iran*

[2]*Department of Physics and Astronomy, Aarhus University, Ny Munkegade 120, DK 8000, Aarhus C., Denmark*

(Received 31 May 2019; published 23 October 2019)

We study the use of ensembles of quantum two-level systems as batteries to store and release radiative energy. Collective coupling to a tuneable cavity mode leads to enhanced charging power and a means to recover the energy on demand in a controllable manner. Individual decay and decoherence of the emitters occur on a much slower timescale, but they gradually cause population of states with lower symmetry and similar to the aging of rechargeable household batteries, they reduce the efficiency of the battery with time.

DOI: 10.1103/PhysRevA.100.043833

I. INTRODUCTION

Quantization of energy levels and quantum phenomena such as coherence and entanglement have been identified as useful ingredients in quantum information processing [1] and sensing [2]. The feasibility and the optimal accomplishment of a range of desired processes with given physical resources are thus being addressed both for their practical relevance and for reasons of more principal and foundational nature.

The ability to operate quantum systems in cycles where coherent processing is separated from state preparation, cooling, and measurements is crucial for numerous quantum technologies with atoms [3], nuclear and electron spin systems [4,5], and superconducting and mechanical systems [6–8]. In addition to their use as quantum registers and quantum memories, one may envision that some quantum degrees of freedom may be excited by external sources to merely form an energy resource that can be released in later, coherent processing steps in the cycle. Experiments in low-temperature environments may draw particular benefits from on-demand release of energy from local energy sources, rather than external driving signals which must be subject to multiple attenuation stages before reaching the target.

As pointed out in recent references [9,10], the power output of thermal machines comprising an ensemble of N particles may experience a cooperative many-body enhancement compared to the output of N incoherent engines, and we observe a similar enhancement of the charging power of a battery formed by a collectively addressed ensemble of two-level quantum systems. A collection of two-level systems, coupled to a single cavity mode, indeed, constitutes an attractive model for such a quantum energy storage device [9,11–15]: (i) The decay via a cavity mode can be Purcell enhanced by several orders of magnitude compared to single emitter radiative decay in free space; (ii) by tuning the cavity frequency and/or damping rate, we can change the lifetime of the excited state of the emitters for charging, storage, and release of energy; (iii) the release of energy proceeds via a single cavity mode, which may coherently couple to other quantum systems.

While the advantages of the Purcell effect and collective coupling and Dicke superradiance for efficient charging have been studied both for excitation by classical and quantum fields [9,10], less effort has been devoted to the fate of the excitation during storage and release of the energy and to the dynamics of the system subject to long sequences of recharging and discharging operations. In this article we study the interplay between the strong collective release of "useful" energy and the (much slower) process of individual decoherence and decay of the individual components of the battery. We quantify how, like household batteries, ensemble quantum batteries age during multiple discharging and recharging steps. The microscopic constituents of the battery, however, do not age and by allowing a sufficient time for discharging of the energy of every single two-level system, the batteries may be rejuvenated to their full capacity. This situation is similar to the one occurring in the use of large spin ensembles as quantum memories [16], where both the treatment of mixed state ensembles by effective pure states of a shortened collective spin and protocols to actively reset fully polarized states are pursued [17].

In Sec. II, we present our physical model and the equations of motion describing the charging, storage, and discharging of energy by the battery. In Sec. III, we present numerical examples of the decay of the battery after a single charging step and we observe its decreasing ability to discharge via the cavity mode after longer storage periods. In Sec. IV, we analyze a mode of operation where the battery is periodically recharged and discharged after only short storage intervals, and we characterize the gradual degradation of its charging capacity. Section V presents our conclusions and a brief outlook.

II. MODEL

Our physical model is illustrated in Fig. 1 and comprises an ensemble of N two-level systems with a closed radiative transition in a single-mode cavity. We assume the systems are identical, i.e., they have no inhomogeneous broadening

*moelmer@phys.au.dk

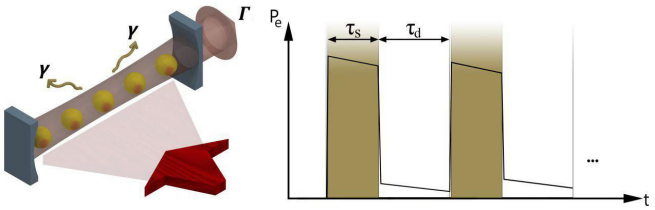

FIG. 1. Left panel: The quantum battery consists of N two-level atoms located in a lossy cavity. The atoms are coherently pumped with a resonant classical (laser or microwave) field and they release their energy by collective coupling to the cavity output field (see main text). Right panel: Battery charging and discharging cycles consist of a rapid excitation pulse, a storage time τ_s in which the atoms decay with individual decay rates γ and a discharging time τ_d in which the atoms are resonant with the cavity mode and experience collective superradiant emission with the Purcell enhanced emission rate Γ.

and they couple with identical coherent coupling to a single mode of the cavity and with identical damping rates to their environment. The systems can be represented as spins that couple to the cavity mode as described by the Hamiltonian ($\hbar = 1$),

$$H_0 = \omega_s \sum_i \sigma_i^z/2 + \omega_c c^\dagger c + ig \sum_i (\sigma_i^- c^\dagger - \sigma_i^+ c), \qquad (1)$$

where σ denotes the Pauli spin, and c and $c^\dagger$ denote the cavity field annihilation and creation operators. ω_s and ω_c are atom and cavity frequency, respectively. The systems are subject to a resonant classical drive described by the Hamiltonian

$$H_1 = A\cos(w_s t) \sum_i \sigma_i^x/2. \qquad (2)$$

Passing to a rotating frame and applying the rotating wave approximation, we obtain the Hamiltonian

$$H = A/2 \sum_i \sigma_i^x/2 + \delta c^\dagger c + ig \sum_i (\sigma_i^- c^\dagger - \sigma_i^+ c), \qquad (3)$$

where $\delta = \omega_c - \omega_s$. The system is subject to damping described by Lindblad terms in the master equation for the total density matrix ρ_T of the cavity and spin quantum state

$$d\rho_T/dt = -i[H, \rho_T] + \sum_{i=1}^{N} \gamma \mathcal{D}[\sigma_i^-]\rho_T + \kappa \mathcal{D}[c]\rho_T. \qquad (4)$$

The superoperator $\mathcal{D}[o]$ is defined as $\mathcal{D}[o]\rho = \{o^\dagger o, \rho\}/2 - o\rho o^\dagger$, and describes the individual decay of the spin system with rate γ and the decay of the cavity mode with rate κ. It is possible to also introduce Lindblad terms that describe individual dephasing and incoherent pumping terms for the spins [18]. Such terms will not be included in our numerical studies.

The classical driving field may act from the side of the cavity or it may be injecting into the cavity through one of the mirrors. After a brief charging period $t \in [0, \tau_c]$, sufficient to perform a Rabi π pulse, the classical pulse is switched off and it is kept off during the subsequent storage time τ_s and discharging time τ_d. Both electronic and nuclear spin transitions and optical atomic transitions can be driven orders of magnitude faster than the excited-state lifetimes of these systems, and we shall assume, $\tau_c \ll \tau_s, \tau_d$.

As the pulsed excitation of the spins can be carried out on a much faster timescale than the decay of the system, rather than solving the equation of motion due to the A terms, we obtain the effect of the pulse by merely applying a 180° spin-rotation around the x axis, allowing analytical treatment of the pulsed excitation.

We also assume the bad cavity limit, i.e., the energy released to the cavity mode escapes from the cavity into a traveling wave field at a high rate $\kappa \gg g$. In this limit, the cavity degrees of freedom can be eliminated and we obtain a closed equation for the reduced density matrix of the spin ensemble, where the most prominent effect is the collectively enhanced superradiant decay process

$$d\rho_S/dt = \sum_{i=1}^{N} \gamma \mathcal{D}[\sigma_i^-]\rho_T + \Gamma \mathcal{D}[S^-]\rho_S. \qquad (5)$$

In Eq. (5), $S^- = \sum_i \frac{1}{2}\sigma_i^-$ is the collective spin lowering operator and $\Gamma = \kappa \frac{g^2}{\kappa^2/4+\delta^2}$ is the Purcell-enhanced emission rate. In this work we shall assume that we can switch the cavity far off resonance and hence suppress the collective decay $\Gamma = 0$. In that situation, the systems only couple to individual loss processes, which we assume to be slow, and the energy can be stored for a time of order $1/\gamma$. When we need the energy, the cavity and the two-level systems are tuned into resonance, so that $\Gamma \gg \gamma$ and the emitters decay predominantly by the collectively and Purcell-enhanced decay via the cavity mode. Such tuning can be carried out on a timescale much faster than the Purcell-enhanced and free-space decay rates of the emitters. One can, e.g., Zeeman shift the transition frequency of atoms in an optical cavity by a magnetic field, and one can tune a superconducting cavity resonance over 100 MHz in a matter of nanosecounds [19,20] much faster than the radiative decay and coupling rates of dopant spin excitations.

Examples of systems relevant for our analysis include the electron spin of nitrogen-vacancy (NV) centers in diamond with a natural lifetime of thousands of seconds, which decreases to only a second when they are brought into resonance with a leaky microwave cavity mode [21]. Optical emitters like ^{87}Sr atoms have an excited state with 150 seconds lifetime in free space [22], and a much shorter lifetime when coupled to a cavity, while the excited-state lifetime of ^{88}Sr [23] and ^{40}Ca [24] are 0.13 and 2.7 ms, respectively, which can be similarly reduced in a cavity for potential application in a battery operating at kHz rate.

The authors of Refs. [9,12,13] studied engines and batteries that benefit from the strong collective coupling of the symmetric states of the ensemble systems. Such systems can be described by collective spin states $|S, M\rangle$, with $S = \frac{N}{2}$ and $S + M$ denoting the number of excited emitters. As we include individual decay of the emitters in this work, the high permutation symmetry of the state is not maintained, and the ensemble will explore a larger Hilbert space. In fact, if the emitters decay with the same rate, their mixed-state density matrix will retain the symmetry under permutation of the emitters, present in the initial ground state, but it will include probability weights on pure states with lower angular momentum quantum number S (e.g., the singlet state of two

spins, which is an antisymmetric state vector, but symmetric when regarded as a component of a density matrix [25]). Rather than treating the decay dynamics by a density matrix on the large Hilbert space of states $|S, M\rangle$, we use the master Eq. (5) to determine equations of motion for mean values of the spin observables $\frac{d}{dt}\langle Q\rangle = \mathrm{Tr}(Q\frac{d}{dt}\rho_S)$. Assuming that all the emitters are equivalent, we thus obtain N identical equations for the mean values

$$\begin{aligned}
\frac{d\langle\sigma_i^z\rangle}{dt} &= -(\gamma+\Gamma)\langle 1+\sigma_i^z\rangle - 2\Gamma(N-1)\langle\sigma_i^+\sigma_j^-\rangle,\\
\frac{d\langle\sigma_i^x\rangle}{dt} &= -\frac{1}{2}(\gamma+\Gamma)\langle\sigma_i^x\rangle + \frac{\Gamma}{2}(N-1)\langle\sigma_i^z\sigma_j^x\rangle,\\
\frac{d\langle\sigma_i^y\rangle}{dt} &= -\frac{1}{2}(\gamma+\Gamma)\langle\sigma_i^y\rangle + \frac{\Gamma}{2}(N-1)\langle\sigma_i^z\sigma_j^y\rangle.
\end{aligned} \tag{6}$$

The cavity field mediates a coupling between the spins and gives rise to terms such as $\langle\sigma_i^z\sigma_j^y\rangle$, which take the same value for all pairs with $i \neq j$.

Equation (6) shows that the rate Γ only appears in combination with the number of emitters N or $N-1$: the "useful" decay through a single cavity mode is both Purcell and collectively enhanced. The equations do not form a closed set, and proceeding to obtain equations for the products of pairs of Pauli operators yields lengthy expressions involving terms with up to three Pauli operators. We approximate such terms by products of lower-order expressions and we thus obtain a closed nonlinear set of equations of motion for the nine variables, $\langle\sigma_i^z\rangle$, $\langle\sigma_i^x\rangle$, $\langle\sigma_i^y\rangle$, $\langle\sigma_i^+\sigma_j^-\rangle$, $\langle\sigma_i^z\sigma_j^z\rangle$, $\langle\sigma_i^+\sigma_j^z\rangle$, $\langle\sigma_i^-\sigma_j^z\rangle$, $\langle\sigma_i^+\sigma_j^+\rangle$, $\langle\sigma_i^-\sigma_j^-\rangle$.

The full set of equations is presented in the Appendix. The solution of these equations represents a second-order mean-field theory without breaking of phase and spatial symmetry of the excitation and spin dynamics. This treatment includes correlations between the emitters, e.g., $\langle\sigma_i^+\sigma_j^-\rangle$, that are not fully accounted for by the mean spin vector components $\langle\sigma_i^z\rangle$, $\langle\sigma_i^x\rangle$, $\langle\sigma_i^y\rangle$.

During the pulsed excitation, the Pauli operators transform as $(\sigma_x^i, \sigma_y^i, \sigma_z^i) \to (\sigma_x^i, -\sigma_y^i, -\sigma_z^i)$ with the resulting consequences for the nine mean values. Hence we shall only retain the damping terms in the nine coupled equations numerically to describe the individual and collective decay of the system between excitation pulses.

III. SINGLE CHARGING, STORAGE, AND RELEASE OF ENERGY FROM THE BATTERY

Figure 2(a) shows the evolution of the total energy stored in the emitters, represented by the z component $\langle S_z\rangle/N = \frac{1}{2}\langle\sigma_z^i\rangle$ of the collective spin. We assume a complete and instantaneous excitation of all emitters at $t = 0$ followed by decay of the stored excitation (red curve) with single-atom decay rate γ. In the figure, we show how tuning of the cavity into resonance with the emitters after six different values of the storage time t_s leads to rapid release of the energy governed by the Purcell-enhanced decay rate $\Gamma = 1600\gamma$ and the collective superradiant emission by $N = 140$ identical emitters. From the equations of motion (6) for $\langle\sigma_z^i\rangle$, we can distinguish the energy released by the individual decay with rate γ and the Purcell- and collectively enhanced rate, proportional

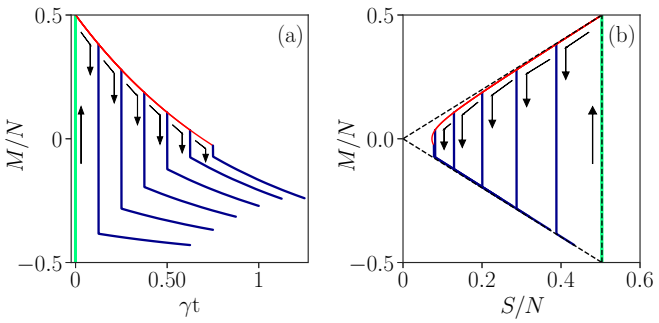

FIG. 2. (a) The mean value of the collective spin component $M = \langle S_z\rangle$ in units of N is shown as a function of time. The heights of the six almost vertical drops show the release of useful energy in units of $N\hbar\omega_s$ if the cavity is brought into resonance with the atoms at the corresponding instants of time. (b) The spin dynamics is represented by time-dependent trajectories in the space of collective spin Dicke quantum numbers S and M, where $S(S+1) = \langle\vec{S}^2\rangle$. The rightmost vertical green line shows the rapid classical excitation, the red curve shows the evolution under the slow individual decay, and the left blue vertical lines show the rapid collective decay, followed by (dashed lines) slow individual decay of the spins. The calculations were done for $N = 140$, $\Gamma = 1600\gamma$ (see main text for details).

to $N\Gamma$. Integrating the later term $\Gamma\langle 1+\sigma_i^z\rangle + 2\Gamma(N-1)\langle\sigma_i^+\sigma_j^-\rangle$ over the duration of the release process yields the energy returned by the battery for useful applications. For our parameters this energy is indiscernible from the total energy lost by the atoms during the rapid decay illustrated by the vertical blue lines in Fig. 2(a). We note that the recent ^{40}Ca experiments [24] have a similar value for $N\Gamma$, and would hence yield similar results.

The dynamics is an interplay of slow individual and rapid collective decay processes, and to explain the results it is convenient to refer to the effective collective spin operators $\vec{\mathrm{S}}^2$ and S_z with quantum numbers S and M (a third quantum number α may be introduced to distinguish degenerate states with the same S and M, but is not needed in the present work). As shown in Refs. [18,26,27] it is possible to describe ensembles of a system with identical individual decay rates in the collective spin basis, but with thousands of emitters or more, we shall use S and M for purely illustrative purposes and extract their average values from the first and second moments determined by our formalism. We have $M = \frac{N}{2}\langle\sigma_i^z\rangle$, while for S, we shall use that $\langle\vec{\mathrm{S}}^2\rangle = \langle S_x^2 + S_y^2 + S_z^2\rangle$ can also be written

$$\langle\vec{\mathrm{S}}^2\rangle = \frac{3}{4}N + \frac{1}{4}\sum_{i\neq j}\left(4\langle\sigma_i^-\sigma_j^+\rangle + \langle\sigma_i^z\sigma_j^z\rangle\right), \tag{7}$$

We extract the value of S by solving the equation $S(S+1) = \langle\vec{\mathrm{S}}^2\rangle$ and we plot the time evolution of the ensemble of emitters as a trajectory in an S, M coordinate systems, restricted by $S \leqslant N/2$ and $|M| \leqslant S$, see Fig. 2(b). In this plot we observe that, during the storage time, the system evolves slowly along the red upper curve which accompanies each loss of an energy quantum by the reduction of S by nearly unity. This is due to the higher degeneracy of the states with the lower S values.

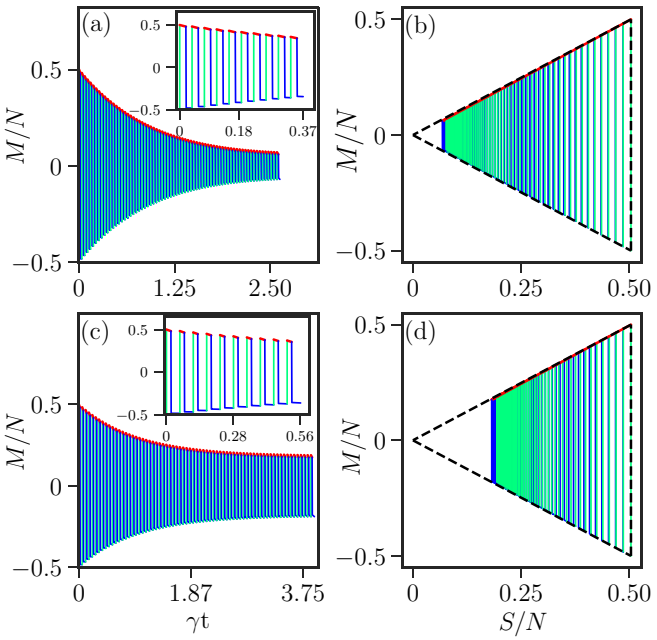

FIG. 3. (a) Excitation of the battery $M = \langle S_z \rangle$ as a function of time during multiple subsequent cycles of charging, storage, and discharging of $N = 140$ emitters with $\Gamma = 1600\gamma$ and $\tau_s = \tau_d = 0.0187\gamma^{-1}$. (b) The variation of M is constrained by the length of the spin S $[S(S+1) = \langle \vec{S}^2 \rangle]$, which shrinks due to the decay of individual emitters. The results suggest that the system reaches a limit cycle of constant charging capacity, where the decrease in S during the storage is balanced by the increase of S at the end of each discharging interval (see text). In panels (c) and (d), the discharging intervals are longer, $\tau_s = 0.0187\gamma^{-1}$ and $\tau_d = 0.0375\gamma^{-1}$, leading to a larger limit cycle value of S and a higher charging capacity of the battery.

For example, when all N atoms are excited, the loss of one excitation by any single emitter yields a state with an occupation $1/N$ on the symmetric state $|S = N/2, M = S - 1\rangle$, while the remaining population is shared among the $N - 1$ states with $S = (N - 1)/2$. For smaller values of S, the individual decay processes occur with increasing probability towards the state with unchanged or increased value of S, explaining the downward bending of the red curve.

It is interesting to note that, while the energy lost during the storage period due to individual decay cannot be recovered, an equivalent amount of energy is trapped in the emitters after the rapid release of energy. This is because the collective emission halts at the state $|S, M = -S\rangle$ which is a subradiant state with respect to the cavity mode, and only an individual decay with rate γ can take the emitters to their ground states [lower dashed line in Fig. 2(b)]. The release of energy into free-space modes surrounding the emitters by the second, slow processes represents an unavoidable loss of useful energy.

IV. MULTIPLE CHARGING, STORAGE, AND RELEASES OF ENERGY FROM THE BATTERY

In Fig. 3 we illustrate the evolution of the excitation of the battery during a repeated sequence of charging, storage, and releases of energy from the battery. All emitter and cavity parameters are the same as in Fig. 2. In each cycle, the system is rapidly inverted by a classical pulse that converts any state component $|S, M = -S\rangle$ into $|S, M = S\rangle$. The emitters subsequently decay slowly during the storage period towards a state characterized by quantum numbers S', M', and when the cavity is tuned on resonance, the emitters quickly decay to $|S', M' = -S'\rangle$. Hereafter they proceed slowly to a state with lower, negative M and hence higher S quantum numbers, $S'', M = -S''$. If the discharging time is short, the coherent excitation pulse brings the system back to an excited state, but with a lower symmetry and a lower value of S than in the previous charging step. Hence less energy is transferred to the battery and less energy will be subsequently released. Like rechargeable household batteries, the quantum battery ages with the number of applications.

We observe that the system reaches a limit cycle value of S and steady state charging capacity of the battery. In this steady state, the mean reduction of S during the storage time equals the increase in S due to individual decay after the very rapid collective release of energy. The system departs from the state $|S, M = S\rangle$ in the storage periods, and the equations of motion for the $\langle \sigma_i^z \rangle$, $\langle \sigma_i^z \sigma_j^z \rangle$, and $\langle \sigma_i^+ \sigma_j^- \rangle$ can be solved to linear order in the storage time τ_s, and thus yield the corresponding average changes of S according to Eq. (5). The steady-state balance yields the condition

$$\left(\frac{2S}{N}\right)^2 - \left(\frac{2S}{N}\right)\left(\frac{\tau_d - \tau_s}{\tau_d + \tau_s} - \frac{4}{N}\right) - \frac{4}{N} = 0. \tag{8}$$

For large N and $\tau_d > \tau_s$, we may ignore the last term, and we find $S = \frac{N}{2}\frac{\tau_d - \tau_s}{\tau_d + \tau_s}$, the charging capacity is linear in the number of spins, with a reduction factor reflecting the reduced symmetry of the state due to the individual decay processes. While this simple expression suggests that $S = 0$ and no energy is stored if the storage and discharge periods are of the same duration, Fig. 3(b) shows that S converges to a finite value. Indeed, for $\tau_d = \tau_s$, the term linear in $\frac{2S}{N}$ disappears in Eq. (8), and we obtain a quadratic equation with the solution $S = \sqrt{N}$.

V. CONCLUSION

In this article we extend the theory of quantum batteries based on ensembles of identical emitters and analyze the interplay between individual and collective decay processes. Using a cavity-enhanced collective coupling mechanism, we can switch the excited state lifetime of the battery by several orders of magnitude between its energy storage mode and release mode. Because of the slow, individual decay processes during energy storage, the battery "ages" and can store less energy in subsequent charging processes. After multiple charging cycles, the battery converges to a limit-cycle charging capacity, depending on the duration of the storage and discharging intervals. Like household batteries, after a complete discharging, the battery regains its initial charging capacity.

The prospects for use as local energy resources and the possibility to address more foundational questions of quantum thermodynamics have spurred interest in quantum batteries and we believe that the present study provides important input to both of these aspects of their behavior and performance. We here consider how individual decay partially degrades

the battery. This analysis can incorporate also the effect of dephasing (which may increase the S quantum number during storage and discharging of the battery an hence yield better limit-cycle performance). An interesting feature of many solid-state spin systems is inhomogeneous broadening, which may cause trapping of energy in subradiant states, but also the release of energy by spin echo techniques. Modelling of the charging and discharging of inhomogeneous systems represents an interesting extension of this work.

ACKNOWLEDGMENTS

F.P. and K.M. acknowledge support from the Villum Foundation, and F.P. acknowledges support from the Ministry of Science, Research, and Technology of Iran.

APPENDIX

We obtain numerical solutions for the dynamics by use of second-order mean-field theory, which supplements the equations of motion for single emitter expectation values $\langle\sigma_i^x\rangle$, $\langle\sigma_i^y\rangle$, $\langle\sigma_i^z\rangle$ with equations for emitter-emitter correlations like $\langle\sigma_i^+\sigma_j^-\rangle$ while higher-order correlations, like $\langle\sigma_i^+\sigma_j^-\sigma_k^z\rangle$ are an approximated by-product of lower-order terms, $\langle ABC\rangle = \langle A\rangle\langle BC\rangle + \langle B\rangle\langle AC\rangle + \langle C\rangle\langle AB\rangle - 2\langle A\rangle\langle B\rangle\langle C\rangle$. This approximation is equivalent to mean-field theory at second order, and it is justified if the observables have relatively small fluctuations around the calculated mean values, i.e., in the limit of many particles. The central limit theorem is often used to argue that the collective observables of many particles have probability distributions well approximated by Gaussians, and for such states, first and second moments, indeed, provide all information about the system. Note that by use of second-order rather than first-order mean-field theory we avoid the need for breaking the phase symmetry, and we recover the collective superradiant decay mechanism through the nonvanishing correlations between the spins. The ensemble is described by the closed set of equations

$$\frac{d\langle\sigma_i^z\rangle}{dt} = -(\gamma+\Gamma)\langle 1+\sigma_i^z\rangle - 2\Gamma(N-1)\langle\sigma_i^+\sigma_j^-\rangle,$$

$$\frac{d\langle\sigma_i^x\rangle}{dt} = -\frac{1}{2}(\gamma+\Gamma)\langle\sigma_i^x\rangle + \frac{\Gamma}{2}(N-1)\langle\sigma_i^z\sigma_j^x\rangle,$$

$$\frac{d\langle\sigma_i^y\rangle}{dt} = -\frac{1}{2}(\gamma+\Gamma)\langle\sigma_i^y\rangle + \frac{\Gamma}{2}(N-1)\langle\sigma_i^z\sigma_j^y\rangle,$$

$$\frac{d\langle\sigma_i^+\sigma_j^-\rangle}{dt} = -(\gamma+\Gamma)\langle\sigma_i^+\sigma_j^-\rangle + \frac{\Gamma}{2}\langle(\sigma_i^z+\sigma_i^z\sigma_j^z)\rangle + \Gamma(N-2)\big(\langle\sigma_i^+\rangle\langle\sigma_j^-\sigma_k^z\rangle + \langle\sigma_j^-\rangle\langle\sigma_i^+\sigma_k^z\rangle + \langle\sigma_k^z\rangle\langle\sigma_i^+\sigma_j^-\rangle - 2\langle\sigma_i^+\rangle\langle\sigma_j^-\rangle\langle\sigma_k^z\rangle\big),$$

$$\frac{d\langle\sigma_i^z\sigma_j^z\rangle}{dt} = -2(\gamma+\Gamma)\langle(1+\sigma_i^z)\sigma_j^z\rangle + 4\Gamma\langle\sigma_i^+\sigma_j^-\rangle - 4\Gamma(N-2)\big(\langle\sigma_i^z\rangle\langle\sigma_j^+\sigma_k^-\rangle + \langle\sigma_j^+\rangle\langle\sigma_i^z\sigma_k^-\rangle + \langle\sigma_k^-\rangle\langle\sigma_i^z\sigma_j^+\rangle - 2\langle\sigma_i^z\rangle\langle\sigma_j^+\rangle\langle\sigma_k^-\rangle\big),$$

$$\begin{aligned}\frac{d\langle\sigma_i^+\sigma_j^z\rangle}{dt} = &-\left(\frac{3}{2}\gamma+\frac{5}{2}\Gamma\right)\langle\sigma_i^z\sigma_j^+\rangle - \left(\gamma+\frac{3}{2}\Gamma\right)\langle\sigma_i^+\rangle - 2\Gamma(N-2)\big(2\langle\sigma_i^+\rangle\langle\sigma_j^+\sigma_k^-\rangle + \langle\sigma_k^-\rangle\langle\sigma_i^+\sigma_j^+\rangle - 2\langle\sigma_i^+\rangle\langle\sigma_j^+\rangle\langle\sigma_k^-\rangle\big)\\ &+\frac{\Gamma}{2}\big(\langle\sigma_i^+\rangle\langle\sigma_j^z\sigma_k^z\rangle + 2\langle\sigma_j^z\rangle\langle\sigma_i^+\sigma_k^z\rangle - 2\langle\sigma_i^+\rangle\langle\sigma_j^z\rangle\langle\sigma_k^z\rangle\big),\end{aligned}$$

$$\begin{aligned}\frac{d\langle\sigma_i^-\sigma_j^z\rangle}{dt} = &-\left(\frac{3}{2}\gamma+\frac{5}{2}\Gamma\right)\langle\sigma_i^z\sigma_j^-\rangle - \left(\gamma+\frac{3}{2}\Gamma\right)\langle\sigma_i^-\rangle - 2\Gamma(N-2)\big(2\langle\sigma_i^-\rangle\langle\sigma_j^-\sigma_k^+\rangle + \langle\sigma_k^+\rangle\langle\sigma_i^-\sigma_j^-\rangle - 2\langle\sigma_i^-\rangle\langle\sigma_j^-\rangle\langle\sigma_k^+\rangle\big)\\ &+\frac{\Gamma}{2}\big(\langle\sigma_i^-\rangle\langle\sigma_j^z\sigma_k^z\rangle + 2\langle\sigma_j^z\rangle\langle\sigma_i^-\sigma_k^z\rangle - 2\langle\sigma_i^-\rangle\langle\sigma_j^z\rangle\langle\sigma_k^z\rangle\big),\end{aligned}$$

$$\frac{d\langle\sigma_i^+\sigma_j^+\rangle}{dt} = -(\gamma+\Gamma)\langle\sigma_i^+\sigma_j^+\rangle + \Gamma(N-2)\big(2\langle\sigma_i^+\rangle\langle\sigma_j^+\sigma_k^z\rangle + \langle\sigma_k^z\rangle\langle\sigma_i^+\sigma_j^+\rangle - 2\langle\sigma_i^+\rangle\langle\sigma_j^+\rangle\langle\sigma_k^z\rangle\big),$$

$$\frac{d\langle\sigma_i^-\sigma_j^-\rangle}{dt} = -(\gamma+\Gamma)\langle\sigma_i^-\sigma_i^-\rangle + \Gamma(N-2)\big(2\langle\sigma_i^-\rangle\langle\sigma_j^-\sigma_k^z\rangle + \langle\sigma_k^z\rangle\langle\sigma_i^-\sigma_j^-\rangle - 2\langle\sigma_i^-\rangle\langle\sigma_j^-\rangle\langle\sigma_k^z\rangle\big).$$

Due to the symmetry of the ensemble, the expressions are the same independent of the value of the index i, the different values of indices i, j, and different values of the three indices.

[1] M. A. Nielsen and I. L. Chuang, *Quantum Computation and Quantum Information* (Cambridge Universty Press, Cambridge, England, 2000).
[2] V. Giovannetti, S. Lloyd, and L. Maccone, Science **19**, 1330 (2004).
[3] A. D. Ludlow, M. M. Boyd, J. Ye, E. Peik, and P. O. Schmidt, Rev. Mod. Phys. **87**, 637 (2015).
[4] P. Cappellaro, L. Jiang, J. S. Hodges, and M. D. Lukin, Phys. Rev. Lett. **102**, 210502 (2009).
[5] J. J. Pla, F. A. Mohiyaddin, K. Y. Tan, J. P. Dehollain, R. Rahman, G. Klimeck, D. N. Jamieson, A. S. Dzurak, and A. Morello, Phys. Rev. Lett. **113**, 246801 (2014).
[6] D. Ristè, C. C. Bultink, K. W. Lehnert, and L. DiCarlo, Phys. Rev. Lett. **109**, 240502 (2012).
[7] M. Stern, G. Catelani, Y. Kubo, C. Grezes, A. Bienfait, D. Vion, D. Esteve, and P. Bertet, Phys. Rev. Lett. **113**, 123601 (2014).
[8] J. Kerckhoff, R. W. Andrews, H. S. Ku, W. F. Kindel, K. Cicak, R. W. Simmonds, and K. W. Lehnert, Phys. Rev. X **3**, 021013 (2013).
[9] X. Zhang and M. Blaauboer, arXiv:1812.10139v1.
[10] Y. Y. Zhang, T. R. Yang, Libin Fu, and X. Wang, Phys. Rev. E **99**, 052106 (2019).
[11] R. Alicki and M. Fannes, Phys. Rev. E **87**, 042123 (2013).
[12] D. Ferraro, M. Campisi, G. M. Andolina, V. Pellegrini, and M. Polini, Phys. Rev. Lett. **120**, 117702 (2018).
[13] F. Campaioli, F. A. Pollock, F. C. Binder, L. Céleri, J. Goold, S. Vinjanampathy, and K. Modi, Phys. Rev. Lett. **118**, 150601 (2017).
[14] G. M. Andolina, M. Keck, A. Mari, M. Campisi, V. Giovannetti, and M. Polini, Phys. Rev. Lett. **122**, 047702 (2019).
[15] W. Niedenzu and G. Kurizki, New J. Phys. **20**, 113038 (2018).
[16] J. H. Wesenberg, A. Ardavan, G. A. D. Briggs, J. J. L. Morton, R. J. Schoelkopf, D. I. Schuster, and K. Mølmer, Phys. Rev. Lett. **103**, 070502 (2009).
[17] C. Grezes, B. Julsgaard, Y. Kubo, M. Stern, T. Umeda, J. Isoya, H. Sumiya, H. Abe, S. Onoda, T. Ohshima, V. Jacques, J. Esteve, D. Vion, D. Esteve, K. Mølmer, and P. Bertet, Phys. Rev. X **4**, 021049 (2014).
[18] Y. Zhang, Y. Xiang Zhang, and K. Mølmer, New J. Phys. **20**, 112001 (2018).
[19] Z. L. Wang, Y. P. Zhong, L. J. He, H. Wang, J. M. Martinis, A. N. Cleland, and Q. W. Xie, Appl. Phys. Lett. **102**, 163503 (2013).
[20] M. Sandberg, C. M. Wilson, F. Persson, T. Bauch, G. Johansson, V. Shumeiko, T. Duty, and P. Delsing, Appl. Phys. Lett. **92**, 203501 (2008).
[21] A. Bienfait, J. J. Pla, Y. Kubo, X. Zhou, M. Stern, C. C. Lo, C. D. Weis, T. Schenkel, D. Vion, D. Esteve, J. J. L. Morton, and P. Bertet, Nature **531**, 74 (2016).
[22] M. A. Norcia, M. N. Winchester, J. R. K. Cline, and J. K. Thompson, Sci. Adv. **2**, e1601231 (2016).
[23] M. A. Norcia and J. K. Thompson, Phys. Rev. X **6**, 011025 (2016).
[24] T. Laske, H. Winter, and A. Hemmerich, Phys. Rev. Lett. **123**, 103601 (2019).
[25] J. Wesenberg and K. Mølmer, Phys. Rev. A **65**, 062304 (2002).
[26] B. Q. Baragiola, B. A. Chase, and J. M. Geremia, Phys. Rev. A **81**, 032104 (2010).
[27] M. Xu, D. A. Tieri, and M. J. Holland, Phys. Rev. A **87**, 062101 (2013).